Stimulated electromagnetic shock radiation characteristics using classical second-order calculations

2004 J. Phys. A: Math. Gen. 37 6837

(http://iopscience.iop.org/0305-4470/37/26/016)

INSTITUTE OF PHYSICS PUBLISHING JOURNAL OF PHYSICS A: MATHEMATICAL AND GENERAL

J. Phys. A: Math. Gen. **37** (2004) 6837–6853 PII: S0305-4470(04)73080-2

Stimulated electromagnetic shock radiation characteristics using classical second-order calculations

A A Risbud

Department of Physics, University of Pune, Pune 411007, India

E-mail: risbud@physics.unipune.ernet.in

Received 6 December 2003, in final form 10 May 2004
Published 16 June 2004
Online at stacks.iop.org/JPhysA/37/6837
doi:10.1088/0305-4470/37/26/016

Abstract

We have investigated the characteristics of stimulated electromagnetic shock radiation (SESR) by using classical, second-order, relativistic calculations. We have derived very compact analytical expressions specifying the electric field components of SESR, which are quite suitable for numerical estimation. We have used, here, a more exact method for solving Lorentz force equations. We have evaluated all the frequency integrals by explicitly imposing the conditions contained in them. Hence we have estimated the SESR effect in different possible physical situations. We have studied, in detail, the important characteristics of SESR, such as frequency up-shift, amplification, energy output and tunability. We have calculated the numerical values of its electric field components and also its output power and frequency. We have shown that very near to the threshold of superphase motion SESR contains two components of frequency 2Ω and 4Ω, which we have named, respectively, SESR-2Ω and SESR-4Ω. The SESR-2Ω is found to be stronger than the SESR-4Ω, with power output $\sim 10^6$ times that of SESR-4Ω. Each of these components is seen to be monochromatic, highly up-shifted in frequency as compared to the incident laser-frequency ω_0 ($10^3 < \Omega/\omega_0 < 10^9$), highly directional, enormously amplified giving power amplification $\sim(10^{27}$ to $10^{44})$ as compared to the Cherenkov radiation (that may be emitted in the absence of the laser, but under the same other conditions), coherent electromagnetic radiation which is also tunable. Because of all these interesting characteristics, SESR may be of use for the generation of high frequency coherent electromagnetic radiation such as x-ray or gamma-ray.

PACS numbers: 41.60.−m, 41.20.−q, 41.60.Cr, 41.60.Bq, 52.59.−f, 41.75.−i

1. Introduction

The head-on collision of a relativistic electron beam, possessing superluminal motion, with a plane electromagnetic wave (laser), gives what is called 'stimulated electromagnetic shock radiation', which we abbreviate as 'SESR'. The dielectric, characterized by the dielectric constant ε which is greater than 1, supports the superluminal or superphase motion of the charge by slowing down the electromagnetic waves and therefore allowing the charge to travel faster than the waves passing through it (superlight charge). When a charged particle moves with a constant superluminal speed in a medium, it emits Cherenkov radiation [1] (CR) which is quite well known. It is given in the form of a cone because the radiated wavelets emitted by the medium under the action of the field of the particle at different points on its path interfere constructively at the Mach angle. It has been extensively studied and also used [2, 3] in high energy physics laboratories. When such a superlight-charged particle is additionally kept under the influence of an external electromagnetic wave, its motion gets modulated and therefore it emits a different radiation called 'stimulated Cherenkov radiation' [4]. The 'Cherenkov lasers' [5, 6], the currently developing devices (in which an electromagnetic wave propagates at a finite angle with an electron beam) for obtaining coherent radiation, are based on the stimulated Cherenkov radiation. The SESR, the subject of the present paper, may be considered as a special case of stimulated Cherenkov radiation in which a particular geometry of the head-on collision of a superlight electron beam with an electromagnetic wave is considered.

The SESR-effect involves occurrence of two phenomena. The first phenomenon is the Doppler shift in frequency of the radiation scattered (the Compton backscattering) from a superlight relativistic electron moving in a dielectric, and the second phenomenon is the formation of a shock by a material body moving at a speed greater than that of the waves it produces in the medium. So, SESR is expected to occur when the Doppler shift in frequency of the radiation scattered in a medium occurs with the Cherenkov radiation condition satisfied giving intense radiation in the form of a shock front, with frequencies shifted markedly from that of the incident wave. In our earlier work [7], we derived analytical results, suitable for estimation of the SESR effect by using classical, second-order, relativistic calculations. The results showed many interesting characteristics of SESR, such as high directionality, enormously large frequency up-shift and also amplification. These characteristics seem to be very useful for the generation of high frequency coherent electromagnetic radiation in a frequency region in which good coherent sources, at present, are not available. Considering its potential use, in the present paper, we study in detail these important characteristics. For that purpose we introduce two changes in the earlier work [7]. Firstly we use a more exact method to solve Lorentz force equations. Secondly, we explicitly impose the conditions implied there on variables of integration while performing the integrations and derive more exact integrated analytical results.

We focus our attention on the most sensitive, nonlinear region of an interaction of the electron with the wave, which is just above but very much in the vicinity of the threshold of superphase motion. Our earlier work [7] has shown a strong SESR effect in this region. However, many aspects of the effect based on higher order calculations yet remain to be studied, such as characteristics of SESR, comparison of SESR effect with other known processes, investigating the question of energy conservation and identifying the source of SESR energy for a better physical understanding of the SESR effect, a feasibility study of its applications such as obtaining high frequency coherent radiation, and its comparison with other existing, high frequency, coherent radiation sources. At present we conduct an in-depth study of different characteristics of SESR.

Firstly we present more exact analytical results and also their comparison with earlier ones. We use here a more accurate method for solving the Lorentz force equation. The method which we used earlier was based [8] on solving the Lorentz force equation in a linear approximation in terms of a small parameter μ. In that method, the solutions for the electron's velocity components were sought in a particular form containing μ. The method was expected to be effectively the same as going to the electron's restframe. But strictly speaking we did not actually transform to the inertial frame moving with the electron. We point out that solving the Lorentz force equations forms the first important step in performing further second-order classical relativistic calculations in the context of SESR. The above method which we used earlier, though somewhat approximate in its first step, was found to be quite successful in tackling rather a complex physical situation of SESR. It also showed very interesting results. Therefore, in the present paper we use a more exact method to solve the Lorentz force equation. We transform all the quantities appearing in the equations to the inertial frame moving with the linear uniform velocity of the electron by using Lorentz transformation equations. We then solve the Lorentz force equation in the electron's rest frame by using a method of linear approximation. The small parameter μ used for its linearization is defined in a peculiar way so that it also judges how much above the threshold of superphase motion the electron is passed through the medium. In order to use SESR for the generation of high frequency coherent radiation, in the present paper we have done a detailed study of the important characteristics of SESR such as output frequency, amplification, directionality, output power and tunability. The analysis is based on the present refined second-order calculations. We also have estimated the values of the frequencies and power obtained from SESR.

Here we want to note one important fact about the experimental work on SESR. There was only one experiment done at the Naval Research Laboratory at Washington, DC [9], way back in 1982, to measure SESR, and it gave a negative result. This may be a reason why there was a decline in further work on SESR. But we want to point out that the theoretical results on which the experiment was designed at that time had the following limitations. Firstly the theories were restricted only to first-order calculations [10–20], which were not enough to reveal all the properties of SESR. Secondly their treatments omitted the most sensitive region of the interaction (which is very near the threshold of superphase motion) in which our more exact, second-order calculations show a very strong effect. Moreover, the results of our earlier work [7] can explain the negative result of the SESR experiment. Our study regarding the variation of the SESR effect with external parameters is quite useful in selecting suitable values for the experimental verification of SESR. Therefore, with new insight provided by the higher order calculations [7], supplemented by our present study, we expect the SESR effect to be experimentally observable. Thus there is a need to perform the experiment to confirm the existence of SESR. Once the experimental verification of SESR is done, it may open up many new avenues of application.

In this paper we present our work in the following four sections. In section 2 we outline the major steps involved in the calculations, and also discuss the implications of the main results of the work. They are given by equations (24), (25) and (26). They specify the electric field components of SESR, in the most compact forms, and they are quite suitable for the numerical estimation of SESR. In section 3 we consider, in detail, the important characteristics of SESR such as its frequency, field strength, power and tunability as quantified by the present results. In section 4 we present the conclusions of our work.

2. Calculations

We consider a relativistic electron possessing a superluminal speed v_0 (exceeding the phase velocity of light), along the positive z-axis, in an infinite medium of unit magnetic permeability. The electric field ($\overline{E_i}$) and the magnetic induction ($\overline{B_i}$) of the plane electromagnetic wave (laser) incident in the opposite direction (head-on collision) is

$$\overline{E_i}(\overline{X}, t) = \hat{y} E_0 \sin(\omega_0 t + k_0 z) \tag{1}$$

$$\overline{B_i}(\overline{X}, t) = n_0 \hat{k}_0 \times \overline{E_i} \tag{2}$$

where $k_0 c = \omega_0 n_0$, c is the speed of light in vacuum and $n_0 = \sqrt{\mu_m \varepsilon}$ is the index of refraction at the incident laser frequency. We consider the case of a non-magnetic ($\mu_m = 1$), non-dispersive medium so that the dielectric constant ε can be taken as a constant and take $v_0 > \frac{c}{n_0}$ or $\varepsilon \beta_0^2 > 1$, where $\beta_0 = \frac{v_0}{c}$.

The motion of the electron of charge $-e$ moving in a dielectric is governed by the incident electromagnetic wave through the Lorentz force [21] given by

$$\overline{F} = \left(-e\overline{D_i} - \frac{e}{c} \bar{v} \times \overline{B}_i \right) = \frac{\mathrm{d}}{\mathrm{d}t} (\gamma m_0 \bar{v}) \tag{3}$$

where displacement vector $\overline{D_i} = \varepsilon \overline{E_i}$, $\bar{v}$ is the velocity of the electron, $\gamma = (1 - \beta^2)^{-1/2}$ and $\beta = v/c$.

The interaction of the electron (possessing superluminal motion) with the counter-propagating electromagnetic wave takes place in a medium whose presence is included in the effect through ε, its dielectric constant. The Lorentz force given by equation (3) specifies the electron's motion as governed by an incident laser.

The presence of the wave imparts an additional oscillatory motion which is superimposed on the uniform rectilinear motion of the electron. The electric field of the wave, $\overline{E_i}$, induces transverse oscillations while the magnetic field, $\overline{B_i}$, is responsible for longitudinal oscillations (w.r.t. $\hat{z}$). For our situation in which $\overline{v_0}$ is perpendicular to $\overline{B_i}$, the magnetic field can deflect the electron only when the electric field displaces it first to give a nonzero component of ($\bar{v} \times \overline{B_i}$) force w.r.t. the frame attached to the electron moving with uniform velocity $\overline{v_0}$. Therefore, inducing longitudinal oscillations is a second-order effect and inducing transverse oscillations is a first-order effect (in the electric field). Here, we assume the parameters of the incident laser to be such that the induced velocity components of the electron's motion are very small compared to the speed with which the electron is incident, and so we can neglect higher order terms. The frequency of these induced oscillations given by the relativistic Doppler effect [21] is

$$\Omega_0' = \omega_0 (1 + \beta_0 n_0) \gamma_0 \tag{4}$$

where $\gamma_0 = \left(1 - \beta_0^2\right)^{-1/2}$.

Thus an oscillatory motion is superimposed on the uniform rectilinear motion of the charge. So, in addition to the uniform velocity $\overline{v_0}$, the charge also possesses acceleration and hence it radiates due to its accelerated motion. The radiation fields (and not just the time-dependent Coulomb field as in the case of CR) of the accelerated charge induce time-dependent polarization in the medium (at a higher frequency). The rapidly changing induced medium polarization gives rise to electromagnetic radiation that is quite different from the normal CR. It is what is called stimulated electromagnetic shock radiation (SESR). The radiation emitted (SESR) can be anticipated to possess frequency up-shift because of the relativistic Doppler effect combined with the Compton backscattering, for the geometry under consideration. The presence of a dielectric medium with $\varepsilon > 1$ not only slows down the electromagnetic waves

passing through it and allows the electron to possess a speed greater than that of the incident and the emitted electromagnetic waves, but also gives out radiation that is confined to a conical region behind it.

Thus, the interaction of the electron possessing superluminal motion with counter-propagating electromagnetic wave gives out SESR. The time varying motion of the electron (under the influence of the incident laser) determines the charge and current densities, whose solutions actually determine the fields of the emitted radiation. That is exactly what we do, here, to get SESR.

Firstly we solve the Lorentz force equation (3) in an inertial frame moving with velocity $\overline{v_0}$ (same as the electron's initial velocity), to get the instantaneous velocity of the charge. Using equations (1) and (2), we write the resulting equation (3) componentwise as

$$m_0 \frac{\mathrm{d}v'_x}{\mathrm{d}t'} = 0 \tag{5}$$

$$m_0 \frac{\mathrm{d}v'_y}{\mathrm{d}t'} = -e\left[\varepsilon E'_i + \frac{n_0}{c} E'_i v'_z\right] \tag{6}$$

$$m_0 \frac{\mathrm{d}v'_z}{\mathrm{d}t'} = e E'_i v'_y \frac{n_0}{c} \tag{7}$$

where a 'prime' denotes the corresponding quantities that are expressed w.r.t. the moving frame. We note here that in equations (5)–(7) $\overline{B_i}$ is not seen because it is expressed in terms of $\overline{E_i}$ using equation (2). We linearize equations (5)–(7) w.r.t. a small parameter, μ, where $v_0 = \frac{c}{n_0}(1+\mu)$ and $\mu \ll 1$ are assumed. This means that the electron is incident with speed slightly above the threshold of superphase motion. This assumption also implies that we are considering the most sensitive nonlinear region of the interaction, which is just above, but very much in the vicinity of the threshold of superphase motion. This region of the interaction is excluded from consideration by all the earlier workers [10–20, 22], and that is one of the reasons why they did not get such a strong effect as we have obtained.

We seek the solution of equations (5)–(7), in the following form:

$$v'_x = 0 \qquad v'_y = \frac{c}{n_0} u_y \mu \qquad v'_z = \frac{c}{n_0} u_z \mu \tag{8}$$

where $\mu \ll 1$, and the initial conditions are at $t' = 0$, $v'_z|_{t'=0} = 0$ and $v'_y|_{t'=0} = 0$.

Substituting velocity components using equation (8) in equations (5)–(7) and keeping only the dominant first-order terms in μ, integrating w.r.t. t' and using the above initial conditions, we get

$$v'_x = 0 \qquad v'_y = \mp \frac{c}{n_0} D' \sin \omega'_0 t' \tag{9}$$

$$v'_z = -\frac{c F' D'}{n_0 4 \omega'_0} (\cos 2\omega'_0 t' + 1) \tag{10}$$

where

$$D' = \frac{e n_0 E'_i \varepsilon}{m_0 c \omega'_0} \qquad \text{and} \qquad F' = \frac{D' \omega'_0}{\varepsilon}.$$

Transforming back to the laboratory frame by using the appropriate Lorentz transformation equations [21], we get the components of the electron's velocity $\bar{v}(t)$ as

$$v_x(t) = 0 \qquad v_y(t) = \mp b_0 \sin \Omega_0 t \qquad v_z(t) = v'_0 - a_0 \cos 2\Omega_0 t \tag{11}$$

where

$$b_0 = \frac{c\varepsilon\beta_i}{\gamma_0} \qquad a_0 = \frac{\varepsilon n_0 c}{4}\beta_i^2 \qquad \beta_i = \frac{eE_0}{m_0 \omega_0 c}$$

$$\Omega_0 = \omega_0(1 + \beta_0 n_0) \qquad \text{and} \qquad v'_0 = v_0 - a_0.$$

Integrating equation (11) w.r.t. t, we get the components of the electron's position, $\bar{R}(t)$ as

$$x(t) = 0 \qquad y(t) = \pm b\cos\Omega_0 t \qquad z(t) = v_0' t - a\sin 2\Omega_0 t \tag{12}$$

where $b = b_0/\Omega_0$ and $a = a_0/2\Omega_0$.

We use the Fourier transform method to solve Maxwell's equations that are governed by the source terms, namely the appropriate charge density $\rho(\bar{r}, t)$ and the current density $\bar{j}(\bar{r}, t)$ given by

$$\rho(\bar{r}, t) = -e\delta(\bar{r} - \bar{R}(t)) \tag{13}$$

$$\bar{j}(\bar{r}, t) = \bar{v}(t)\rho(\bar{r}, t). \tag{14}$$

We substitute, respectively, for the electron's velocity and position from equations (11) and (12) in equations (13) and (14); and perform calculations correct up to the second-order terms in β_i (for details see [7]), to get the following expressions for the electric field components of SESR.

$$\begin{aligned} E_z(\bar{r}, t) = \frac{e}{2c^2}\int_{-\infty}^{+\infty} \omega\,\mathrm{d}\omega\,\mathrm{e}^{\mathrm{i}\omega t}\Bigg\{ & H_0^{(2)}(\rho A)\left(1 - \frac{c^2 k}{\varepsilon\omega v_0'}\right)\left(1 - \frac{b^2A^2}{4}\right)\mathrm{e}^{-\mathrm{i}kz} \\ & - H_0^{(2)}(\rho A_\pm)\left[\left(1 - \frac{c^2 k_\pm}{\varepsilon\omega v_0'}\right)\left(\frac{b^2A_\pm^2}{8} \pm \frac{ak_\pm}{2}\right) - \frac{2a\Omega_0}{v_0'}\right]\mathrm{e}^{-\mathrm{i}k_\pm z} \\ & + \frac{b}{2}\,\mathrm{e}^{\mp\mathrm{i}\pi/2} H_0^{(2)}(\rho A_\pm')\left[A_\pm'\left(1 - \frac{c^2 k_\pm'}{\varepsilon\omega v_0'}\right)\right]\mathrm{e}^{-\mathrm{i}k_\pm' z}\Bigg\} \end{aligned} \tag{15}$$

$$\begin{aligned} E_\rho(\bar{r}, t) = \frac{e}{2\varepsilon v_0'}\int_{-\infty}^{+\infty} \mathrm{d}\omega\,\mathrm{e}^{\mathrm{i}\omega t}\Bigg\{ & -A H_0^{(2)}(\rho A)\left(1 - \frac{b^2A^2}{4}\right)\mathrm{e}^{-\mathrm{i}kz} \\ & + \frac{A_\pm}{2v_0'} H_0^{(2)}(\rho A_\pm)\left[\frac{b^2A_\pm^2}{4} \pm ak_\pm \mp \frac{b^2\varepsilon\Omega_0}{2c^2}\omega\right]\mathrm{e}^{-\mathrm{i}k_\pm z} \\ & + \frac{b\varepsilon}{2}\,\mathrm{e}^{\mp\mathrm{i}\pi/2} H_0^{(2)}(\rho A_\pm')\left[\frac{1}{\varepsilon} \pm \frac{\Omega_0}{c^2}\omega\right]\mathrm{e}^{-\mathrm{i}k_\pm' z}\Bigg\} \end{aligned} \tag{16}$$

$$\begin{aligned} E_\phi(\bar{r}, t) = \frac{\pi e}{2\varepsilon v_0'}\int_{-\infty}^{+\infty} \mathrm{d}\omega\,\mathrm{e}^{\mathrm{i}\omega t}\Bigg\{ & H_0^{(2)}(\rho A_\pm)\left[\frac{b^2A_\pm^2}{8} \pm \frac{ak_\pm}{4}\right]\mathrm{e}^{-\mathrm{i}k_\pm z} \\ & + \frac{b}{2}\,\mathrm{e}^{\mp\mathrm{i}\pi/2} A_\pm' H_0^{(2)}(\rho A_\pm')\,\mathrm{e}^{-\mathrm{i}k_\pm' z}\Bigg\} \end{aligned} \tag{17}$$

where $\pm$ terms with $\pm$ suffixes are written together for convenience, but are to be read as separate terms, $H_0^{(2)}(\rho A)$ is the Hankel function of second kind, and the position vector $\bar{r}$ is expressed in cylindrical coordinates as $\bar{r}(\rho, \phi', z)$,

$$a = \frac{e^2E_0^2n_0^3}{16m_0^2\omega_0^3 c} \qquad b = \frac{eE_0n_0^2}{2m_0\omega_0^2\gamma_0} \qquad k = \frac{\omega}{v_0'} \qquad k_\pm = \frac{\omega \pm 4\Omega_0}{v_0'} \qquad k_\pm' = \frac{\omega \pm 2\Omega_0}{v_0'}$$

$$v_0' = v_0 - 2a\Omega_0 \qquad A^2 = \frac{\varepsilon\omega^2}{c^2} - k^2 \qquad A_\pm^2 = \frac{\varepsilon\omega^2}{c^2} - k_\pm^2 \qquad A_\pm'^2 = \frac{\varepsilon\omega^2}{c^2} - k_\pm'^2$$

$$\mathrm{Re}\,A > 0 \qquad \mathrm{Re}\,A_\pm > 0 \qquad \text{and} \qquad \mathrm{Re}\,A_\pm' > 0.$$

In equations (15)–(17) the terms which contain a factor b specify the first-order effect, and they show the shift of frequency by a factor $\pm 2\Omega_0$. We called the effect specified by the first-order terms SESR-2Ω. The terms appearing in the above equations that contain factors

a and b^2 correspond to the second-order effect. They show a frequency shift by a factor $\pm 4\Omega_0$. We have named them SESR-4Ω. The terms having no shift in frequency are identified as representing the normal CR but with amplitude modified because of the presence of the electromagnetic wave. We have called them CR-like SESR.

Here we point out that the parameters a and b that appeared in our earlier paper [7] were found to be smaller, in comparison with their values specified above, by factors $\sim 1/\left(16\gamma_0^3\right)$ and $\sim 1/\left(4\gamma_0^2\right)$, respectively. The reason is that earlier we used a different approach to the problem, in which we evaluated the electron's instantaneous velocity in the laboratory frame of reference; while in the present work we have used the electron's rest frame for our calculations. We also point out that the above inequalities were not written explicitly in the earlier paper [7], though they were assumed to be satisfied there.

We further note that the above relations following equations (15)–(17), relating k, $k_\pm$, $k'_\pm$ with ω, can be put in a general form as given below:

$$\omega = k v'_0 + 2s\Omega_0 \tag{18}$$

where $s = 0, \pm 1, \pm 2$.

Equation (18) is nothing but the resonance condition specifying the frequencies of the emitted radiation (SESR). It reduces to the condition for the appearance of the Cherenkov wave [23] for $s = 0$, when the incident laser is weak enough to satisfy the condition $2a\Omega_0/v_0 \ll 1$.

For $s \neq 0$, by substituting $k = \omega n_0/c$ in equation (18) we can express the above resonance condition as

$$\omega = \frac{2s\Omega_0}{1 - \beta_0 n_0 + \frac{2a\Omega_0 n_0}{c}}. \tag{19}$$

For $s = +1$ and $+2$, equation (19) corresponds to the conditions for the appearance of the normal Doppler frequencies for which the restriction $\beta_0 n_0 < 1$ is applicable; while for $s = -1$ and -2, it gives the emission of anomalous Doppler [23, 24] frequencies for which the condition for superphase motion $\beta_0 n_0 > 1$ needs to be satisfied. In both cases other parameters are such that they satisfy the condition $\frac{2a\Omega_0 n_0}{c} \ll 1$.

Thus, for $s = -1$ and -2, equation (19) specifies the frequencies for the appearance of SESR-2Ω and SESR-4Ω, respectively. The resonance condition given by equation (19) clearly shows the additional (w.r.t. Ω_0) frequency up-shift $\sim 1/|1 - \beta_0 n_0|$, which in our case is very large, since we are considering the situation in which $(\beta_0 n_0 - 1) = \mu \ll 1$. This is exactly the frequency up-shift identified by us in the earlier paper [7] from the integrated expressions of equations (15)–(17). It was specified by the phase factors appearing in equations (35)–(37) of our earlier work and pointed out on page 7 of the earlier work [7]. Getting such a large frequency up-shift is a very important property of SESR, which may be quite useful in practice. We consider it in detail later in section 3.

To get expressions that are more suitable for numerical estimation of SESR fields, we integrate equations (15)–(17). For that we take the asymptotic form of Hankel functions and use the stationary phase method. We note that the conditions, namely $\mathrm{Re}\, A_\pm > 0$ and $\mathrm{Re}\, A'_\pm > 0$ appearing in the equations (15)–(17), contain the dependence of ω. But earlier [7] they were not imposed while calculating the ω integrals. The imposition of the above conditions leads to some changes in the integrated expressions which we present below.

To perform the integrations w.r.t. ω, we first rewrite equations (15)–(17) showing their ω dependence explicitly. We use the following approximation formula given by the method of

stationary phase [7],

$$\int_{\omega_1}^{\omega_2} \mathrm{d}\omega\, \Phi(\omega)\, \mathrm{e}^{\mathrm{i}f(\omega)} = \frac{\sqrt{2\pi}\,\Phi(\omega_0')}{\sqrt{|f''(\omega_0')|}} \exp\left(\mathrm{i}f(\omega_0') \pm \mathrm{i}\frac{\pi}{4}\right) \tag{20}$$

where ω_0' represents the root of the equation,

$$f'(\omega_0') = \left.\frac{\mathrm{d}f}{\mathrm{d}\omega}\right|_{\omega=\omega_0'} = 0 \tag{21}$$

which lies within the range of integration and where the upper or lower sign is to be taken in the exponential as $f''(\omega_0')$ is positive or negative.

We identify $f(\omega)$ for the different ω integrals contained in equations (15)–(17) and use them to solve equation (21), under the conditions $\mathrm{Re}\, A_\pm > 0$ and $\mathrm{Re}\, A'_\pm > 0$, and get the following roots:

$$\omega_0' = \frac{b_1 + \Delta}{2a_1} \qquad \text{for} \quad \mathrm{Re}\, A_+ > 0 \tag{22}$$

$$\omega_0'' = \frac{-b_1 + \Delta}{2a_1} \qquad \text{for} \quad \mathrm{Re}\, A_- > 0 \tag{23}$$

where

$$\Delta = \sqrt{b_1^2 + 4a_1d_1} \qquad d_1 = \frac{4c_1t'^2 + b_1^2\rho^2}{4(t'^2 - \rho^2a_1)} \qquad a_1 = \frac{\varepsilon\beta_0'^2 - 1}{v_0'^2} \qquad b_1 = \frac{8\Omega_0}{v_0'^2} \qquad c_1 = \frac{16\Omega_0^2}{v_0'^2}.$$

The roots of equation (21) under the condition $\mathrm{Re}\, A'_\pm > 0$ can be written by replacing b_1 by $\frac{b_1}{2}$ and c_1 by $\frac{c_1}{4}$ in equations (22) and (23). Hence using equations (20), (22) and (23), we evaluated all the integrals that are contained in equations (15)–(17) and obtained the final result as given below

$$\begin{aligned} E_z(\bar{r}, t) = \frac{-e}{2c^2}\Bigg\{ & \alpha_9 \frac{1}{\sqrt{\rho}(t' - \rho\sqrt{a_1})^{3/2}} + \frac{\eta_1}{\rho} \exp\left(-\mathrm{i}\frac{4\Omega_0\rho\eta_1}{v_0'\sqrt{\mu'}}\right) \\ & \times \alpha_{11} \sin\left(\frac{4\Omega_0t'\eta_2}{\varepsilon\beta_0'^2 - 1} - \frac{4\Omega_0z}{v_0'}\right) + \frac{\eta_1}{\left(\frac{t'^2}{a_1} - \rho^2\right)^{1/2}} \exp\left(-\mathrm{i}\frac{2\Omega_0\rho}{v_0'\sqrt{\mu'}}\eta_1\right) \\ & \times \alpha_{13} \cos\left(\frac{2\Omega_0t'\eta_2}{\varepsilon\beta_0'^2 - 1} - \frac{4\Omega_0z}{v_0'}\right)\Bigg\} \end{aligned} \tag{24}$$

$$\begin{aligned} E_\rho(\bar{r}, t) = \frac{e}{2c^2}\Bigg\{ & \alpha_{14} \frac{1}{\sqrt{\rho}(t' - \rho\sqrt{a_1})^{3/2}} + \frac{\eta_1}{\left(\frac{t'^2}{a_1} - \rho^2\right)^{1/2}} \exp\left(-\mathrm{i}\frac{4\Omega_0\rho}{v_0'\sqrt{\mu'}}\eta_1\right) \\ & \times \alpha_{16} \sin\left(\frac{4\Omega_0t'\eta_2}{\varepsilon\beta_0'^2 - 1} - \frac{4\Omega_0z}{v_0'}\right) + \frac{\eta_1}{\rho} \exp\left(-\mathrm{i}\frac{2\Omega_0\rho}{v_0'\sqrt{\mu'}}\eta_1\right) \\ & \times \alpha_{18} \cos\left(\frac{2\Omega_0t'\eta_2}{\varepsilon\beta_0'^2 - 1} - \frac{2\Omega_0z}{v_0'}\right)\Bigg\} \end{aligned} \tag{25}$$

$$\begin{aligned} E_\phi(\bar{r}, t) = \frac{e}{2c^2}\Bigg\{ & \frac{\eta_1}{\rho} \exp\left(-\mathrm{i}\frac{4\Omega_0\rho}{v_0'\sqrt{\mu'}}\eta_1\right) \alpha_{20}\, \mathrm{e}^{-\mathrm{i}\pi/2} \cos\left(\frac{4\Omega_0t'\eta_2}{\varepsilon\beta_0'^2 - 1} - \frac{4\Omega_0z}{v_0'}\right) \\ & + \frac{\eta_1}{\left(\frac{t'^2}{a_1} - \rho^2\right)^{1/2}} \exp\left(-\mathrm{i}\frac{2\Omega_0\rho}{v_0'\sqrt{\mu'}}\eta_1\right) \alpha_{22}\, \mathrm{e}^{\mathrm{i}\pi/2} \sin\left(\frac{2\Omega_0t'\eta_2}{\varepsilon\beta_0'^2 - 1} - \frac{2\Omega_0z}{v_0'}\right)\Bigg\} \end{aligned} \tag{26}$$

where

$$\rho < \frac{t'}{\sqrt{a_1}} \qquad \eta_1 = \frac{\rho}{\left(\frac{t'^2}{a_1} - \rho^2\right)^{1/2}} \qquad \eta_2 = 1 \pm \frac{\beta_0' t' \sqrt{\varepsilon}}{\sqrt{a_1}\left(\frac{t'^2}{a_1} - \rho^2\right)^{1/2}} \qquad t' = t - \frac{z}{v_0'}$$

$$\alpha_9 = \frac{\mu'}{4(a_1)^{1/4}} \qquad \mu' = 1 - \frac{1}{\varepsilon\beta_0'^2} \qquad \alpha_{11} = \frac{2b_1\alpha_3}{a_1^{3/2}} \qquad \alpha_3 = \left(\frac{b^2 b_1 \Omega_0}{2\varepsilon\beta_0'^2} - \frac{4a\Omega_0}{v_0'\varepsilon\beta_0'^2} - \frac{b^2 c_1 \mu'}{8}\right)$$

$$\alpha_{13} = 2\alpha_8\left(\frac{b_1^2}{16a_1} + \frac{c_1}{4}\right)^{1/2} \qquad \alpha_8 = \frac{8b\Omega_0}{\varepsilon\beta_0'^2\sqrt{a_1}} \qquad \alpha_{14} = \frac{c a_1^{1/4}}{4\varepsilon\beta_0'} \qquad \alpha_{16} = \frac{64\Omega_0^2|\alpha_4|}{\sqrt{\varepsilon}\beta_0' a_1^2 v_0'^4}$$

$$\alpha_{20} = \frac{4\pi v_0'|\alpha_7|}{\varepsilon\beta_0'^2\sqrt{a_1}} \qquad \alpha_4 = \left(\frac{a}{v_0'} - \frac{b^2 b_1}{4} - \frac{b^2\varepsilon\Omega_0}{2c^2}\right) \qquad \alpha_{18} = \frac{4b_1 b\Omega_0}{v_0' a_1^{3/2}}$$

$$\alpha_7 = \left(\frac{a\Omega_0}{v_0'} - \frac{b^2 c_1}{8}\right)$$

and

$$\alpha_{22} = \frac{\pi b v_0'}{\varepsilon\beta_0'^2\sqrt{a_1}}\left(\frac{b_1^2}{16a_1} + \frac{c_1}{4}\right)^{1/2}.$$

The most compact, integrated expressions given by equations (24)–(26) specify the components of the SESR fields. They contain all the characteristics of SESR. The first terms of equations (24) and (25) containing the factors α_9 and α_{14} represent the field components of CR-like SESR. In the absence of the laser (which implies $a = 0 = b$) they reduce exactly to the field components of normal CR [25]. The second terms of equations (24), (25) and the first term of equation (26), which contain in phase a factor of $4\Omega_0$, represent SESR-4Ω. The third terms appearing in equations (24) and (25); and the second term of equation (26) which contain a factor of $2\Omega_0$ in phase give SESR-2Ω contributions.

Equations (24)–(26) given above are simpler than equations (35)–(37) of the earlier results [7] because the terms containing the factors, namely $\alpha_{10}, \alpha_{15}, \alpha_{17}$ and α_{21}, are found not to be contributing to the final result here. This is due to the imposition of the conditions, namely $\mathrm{Re}\, A > 0$, $\mathrm{Re}\, A_\pm > 0$ and $\mathrm{Re}\, A'_\pm > 0$.

As compared to the earlier factors [7], in the present work the coefficients α_{13} and α_{18} show small multiplying factors (namely 4 and 16, respectively), but the coefficients α_{20}, α_{22} and α_{16} are seen to have large multiplying factors (namely $16\gamma_0^2 v_0'$, $2\gamma_0 v_0'$ and $64\gamma_0/\left(c\beta_0'^5\sqrt{a_1}\right)$, respectively). All SESR components show an additional multiplying factor η_1. The effect of these modifications will be reflected in the SESR-field values which we shall show later in section 3.

We note the presence of a factor $\mathrm{i} = \sqrt{-1}$ in the exponentials of equations (24)–(26). It results in the propagation of the field components (and not growth) along the ρ-direction. In our earlier work [7], exponential growth along ρ appeared because of not explicitly imposing the conditions (which were contained in their equations (B6) and (B7), in which (B5) was used), namely $\mathrm{Re}\, A_\pm > 0$ and $\mathrm{Re}\, A'_\pm > 0$, while integrating w.r.t. ω. Equations (24)–(26) show additional factors in phase, namely η_1 and η_2. Their contribution is judged by noting that $\rho = t'/\sqrt{a_1}$ represents the CR-cone, and so the condition $\rho < t'/\sqrt{a_1}$ confines SESR to the region inside the CR-cone; and that their maximum values can be expressed in terms of the CR-cone angle, θ_c, as $\eta_1 \sim \tan\theta_c = \sqrt{\varepsilon\beta_0'^2 - 1}$, $\eta_2 \sim \left(\pm\varepsilon\beta_0'^2 + 1\right)$. Therefore, we find that the changes in phase factors due to the appearance of η_1 and η_2 are quite small.

These changes in phase get reflected in the propagation vectors of SESR-2Ω (i.e. $\bar{k}_{2\Omega}$) and SESR-4Ω (i.e. $\bar{k}_{4\Omega}$). The ρ and the z components of $\bar{k}_{2\Omega}$ and $\bar{k}_{4\Omega}$ can be identified from

the coefficients of ρ and z, which appear in the phase factor, respectively, of SESR-2Ω terms and SESR-4Ω terms given by equations (24)–(26). With respect to $\hat{z}$, for both SESR-2Ω and SESR-4Ω, they can be seen to satisfy the following relation:

$$\theta = \tan^{-1}\left(\frac{k_\rho}{k_z}\right) \sim \tan^{-1}\left(1 - \frac{1}{\beta_0 n_0}\right) \to 0 \tag{27}$$

as $\beta_0 n_0 - 1 = \mu \ll 1$.

Equation (27) shows that both SESR-2Ω and SESR-4Ω radiation are emitted in the forward direction making a very small angle w.r.t $\hat{z}$. The angle of their emission θ reduces as the threshold of superphase motion is approached from inside the CR cone by reducing the electron velocity (therefore energy) but remaining in the region of the superluminal motion.

The coefficient of time t in phase can be identified as the frequency of the emitted modes of the radiation. For SESR-4Ω and SESR-2Ω they are given, respectively, as

$$\frac{4\Omega_0\eta_2}{\varepsilon\beta_0'^2 - 1} \qquad \text{and} \qquad \frac{2\Omega_0\eta_2}{\varepsilon\beta_0'^2 - 1}.$$

Substituting for η_2, they give the following four possible frequency components:

$$\frac{2\Omega_0\left(1+\varepsilon\beta_0'^2\right)}{n_0\beta_0' - 1} \qquad -2\Omega_0 \qquad \frac{\Omega_0\left(1+\varepsilon\beta_0'^2\right)}{n_0\beta_0' - 1} \qquad -\Omega_0.$$

The Ω_0 and $2\Omega_0$ components can be identified, respectively, as the Doppler-shifted frequency component and its first harmonic both propagating along the $-\hat{z}$ direction. As $\varepsilon\beta_0'^2 \sim 1$, $\beta_0' \sim \beta_0$, the remaining two components with frequencies $\sim\frac{2\Omega_0}{B_0 n_0 - 1}$ and $\sim\frac{4\Omega_0}{\beta_0 n_0 - 1}$ are, respectively, the enormously up-shifted (since the factor in the denominators, $\beta_0 n_0 - 1 = \mu \ll 1$) frequency components due to SESR-2Ω and SESR-4Ω which propagate along the $+\hat{z}$ direction.

In our earlier work [7], the ρ-dependence of the SESR-field components was kept aside while calculating the numerical estimates of SESR fields. Here we include it through the factor η_1. We calculate Poynting's vector to find the radiated power through SESR. This is what is shown in the next section 3.

3. Characteristics

In this section we consider, in detail, the important characteristics of SESR, such as its frequency, field strength and power as specified by the results of the present calculations. Its numerical estimation is important since it gives a clear understanding of the effect of SESR.

3.1. Frequency output

Firstly we consider the frequency emitted by the SESR effect. The output frequencies from SESR-2Ω and SESR-4Ω are given by equation (19) with $s = -1$ and $s = -2$, respectively. Using $\frac{2a\Omega_0 n_0}{c} \ll 1$, which is valid in our case, equation (19) gives the values of the frequencies of SESR-2Ω and SESR-4Ω, respectively, as 2Ω and 4Ω, where $\Omega = \Omega_0/(\beta_0 n_0 - 1)$. These are exactly the frequencies identified and shown by the coefficients of t in the phase factors of our final results given by equations (24)–(26). They show that the SESR frequency depends upon the laser frequency (ω_0), electron speed (β_0) and the refractive index of the material (n_0) which supports the superluminal motion. Their choice is very important because the up-shift from the incident laser frequency is mainly decided by the factor $(\beta_0 n_0 - 1)^{-1}$. For the electron to possess superphase motion the condition $\beta_0 n_0 > \sim 1$ needs to be satisfied. So the electron energy is to be chosen such that it is above the threshold for a given n_0. Thus the frequency up-shift depends upon how much above from the threshold value the electron is made to move.

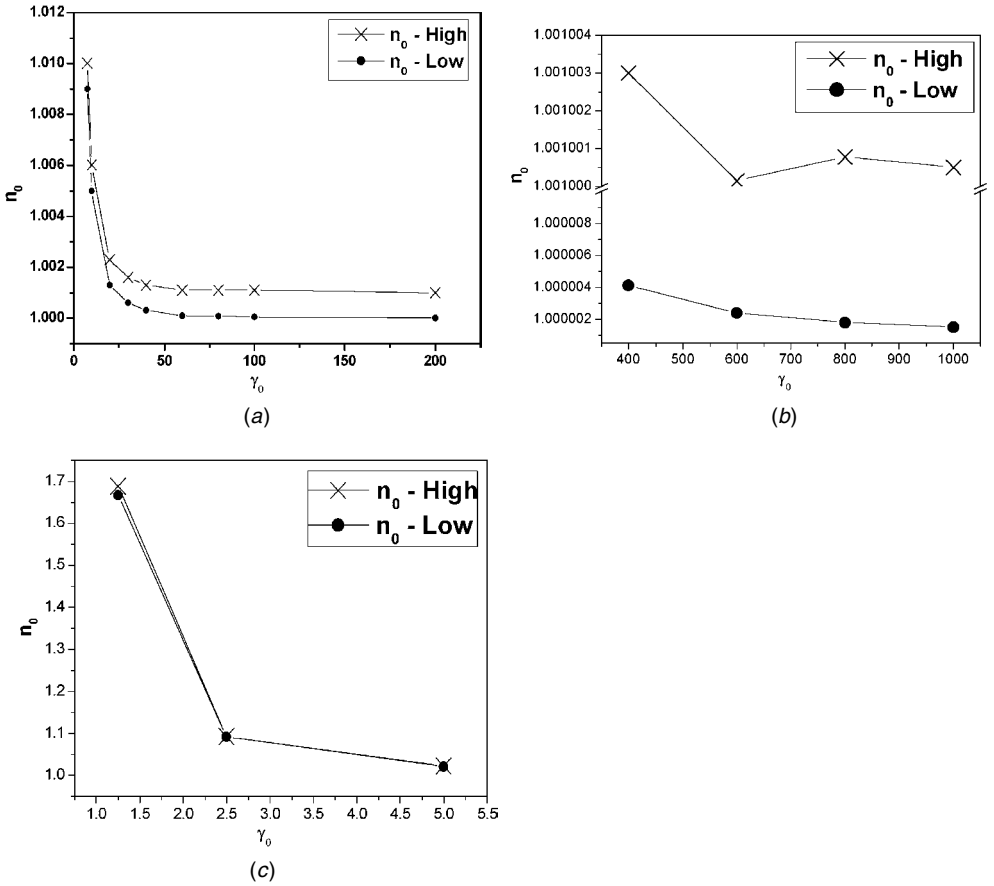

Figure 1. The ranges of refractive index-values (n_0-high to n_0-low), for which the SESR effect is possible for different γ_0-values.

We recall that the parameter μ (used in the linearizing procedure applied to the Lorentz force equation (3)) equals $(\beta_0 n_0 - 1)$, and that the assumption $\mu \ll 1$ also needs to be satisfied for our theory to remain applicable. Therefore, the up-shift can be extremely high if we are able to choose the appropriate material for which the condition for the electron's superphase motion is just satisfied. The values of the parameters β_0 and n_0 need to be controlled so nicely that the superphase motion continues to be very near to its threshold.

Thus the laser frequency, electron speed (energy) and refractive index of the material are the three controlling parameters available to obtain the desired frequency output by SESR. In order to know how to choose their values, we calculate them by taking a range of μ-values within which our approximations remain valid. We consider the range of μ-values from 10^{-6} to 10^{-3}, which gives the frequency up-shift in the range of 10^7–10^3. From equation (19), the actual values of the SESR frequencies are given approximately as $\frac{4\omega_0}{\mu}$ and $\frac{8\omega_0}{\mu}$, because $\beta_0 n_0 \sim 1$ and $\Omega_0 \sim 2\omega_0$. As $\mu = \beta_0 n_0 - 1$, for different values of electron beam energy (γ_0), we calculate the refractive index (n_0) that is required for a given μ. In figures 1(a), (b) and (c), we show the allowed ranges (n_0-high to n_0-low) within which the values of n_0 need to be chosen for different values of γ_0 obtained by considering the values of $\mu = 10^{-3}$ and $\mu = 10^{-6}$ to get the predicted SESR effect.

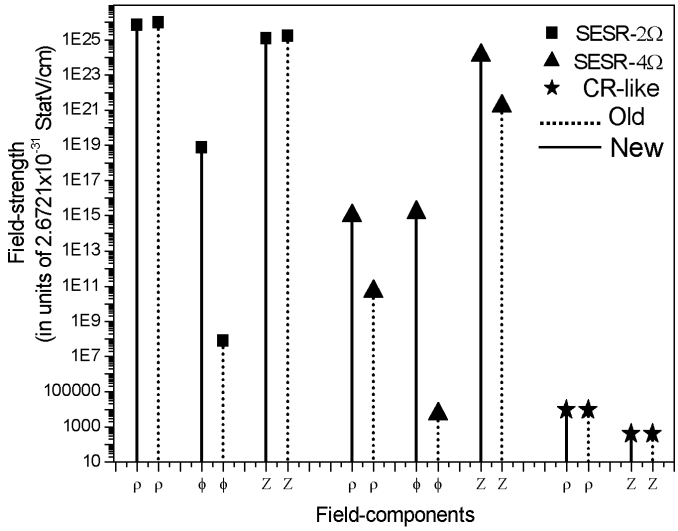

Figure 2. The electric field components (ρ, ϕ and z) of the emitted radiation due to the SESR effect (2Ω, 4Ω and CR-like) for $\gamma_0 = 18.29$, $E_0 = 3 \times 10^5$ StatV cm^{-1}, $\omega_0 = 5 \times 10^{15}$ Hz and $n_0 = 1.0025$ (for $\mu = 1 \times 10^{-3}$).

Looking at their values from figures 1(a) and (b), we can say that for high-energy electron beams ($\gamma_0 > \sim 10$) gaseous media need to be chosen. Solids (such as polyethylene) may be chosen only for lower electron beam energies ($\gamma_0 < \sim 5$) as shown in figure 1(c). The choice of an appropriate material that makes the required superluminal motion possible (by remaining very near to the threshold of superphase motion) for available high energy electron beams is an important issue, and it needs to be investigated further for practical applications of the SESR-effect.

We note that the choice of the laser frequency ω_0 decides the lower limit of the frequency output. If we choose ω_0 in IR, the frequency of SESE-2Ω will be in the x-ray or gamma-ray region. In principle, frequency up-shift can be as high as 10^7 (or even more, if we are able to choose smaller μ), but in practice dispersive properties of the medium may put a lower limit to how close we can approach to the threshold value and be able to maintain the required conditions. We need to know the response of the dielectric for the incident laser frequency ω_0, and also the output frequencies 2Ω and 4Ω. We proceed to estimate the field amplitudes of SESR.

3.2. Field strength

Here, we calculate the values of the field components of SESR and compare them with the earlier ones. We show the results graphically for easy comparison.

Using the results specified by equations (24)–(26), we calculate the electric field components of SESR for $\gamma_0 = 18.29$, $E_0 = 3 \times 10^5$ StatV cm^{-1}, $\omega_0 = 5 \times 10^{15}$ Hz and $n_0 = 1.0025$ (for $\mu = 1 \times 10^{-3}$) and denote them in figure 2 by 'new'; while the corresponding components calculated in our earlier work [7] we show by 'old'. We express all the field components in units of $(e/2c^2) = 2.6721 \times 10^{-31}$ StatV cm^{-1}.

We note from figure 2 that for SESR-2Ω, ρ and z are the two dominant field components, while for SESR-4Ω only the z-component is dominant and that the SESR effect is very large as compared to CR-like SESR. In units of $e/2c^2$ the field strength of CR-like SESR is seen

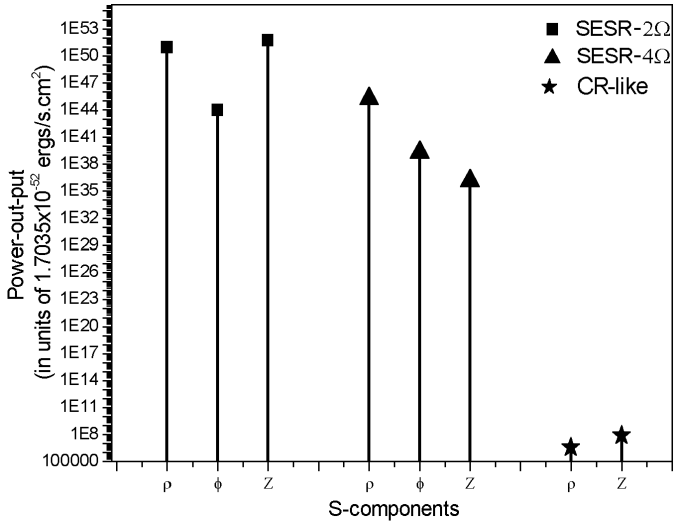

Figure 3. The ρ-, ϕ- and z-components of Poynting's vector $\overline{S} = \frac{c}{4\pi}(\overline{E} \times \overline{H})$, in units of $\frac{c}{4\pi}(\frac{e}{2c^2}) = 1.7035 \times 10^{-52}$ ergs (s cm)$^{-2}$, for $\gamma_0 = 18.29$, $n_0 = 1.0025$, $E_0 = 3 \times 10^5$ StatV cm^{-1}, $\omega_0 = 5 \times 10^{15}$ Hz.

to be $\sim 10^2$–10^3 while the remaining (new) SESR components lie within the range of 10^{14}–10^{25}. We also see from figure 2 that there is a considerable enhancement $\sim$11–12 orders of magnitude in new ϕ-components. But it is of no significance because the ϕ-components are negligibly small in comparison with the corresponding ρ- and z-components The 'new' ρ- and z-components of SESR-2Ω are almost the same as their 'old' values. For SESR-4Ω, the ρ-component increases by four orders and the z-component increases by three orders of magnitude. Thus, the present refined calculations show a large increase in SESR-4Ω, while almost no change in SESR-2Ω.

3.3. Power output

In order to estimate the radiated energy output, we calculate the Poynting's vector $\overline{S} = \frac{c}{4\pi}(\overline{E} \times \overline{H})$, where $\overline{H} = (\hat{k} \times \overline{E})n_0$, and $\overline{E}$ is given by equations (24)–(26). We assume that the parameters are the same as taken in figure 2, e.g., $\gamma_0 = 18.29$, $n_0 = 1.0025$, $E_0 = 3 \times 10^5$ StatV cm^{-1} and $\omega_0 = 5 \times 10^{15}$ Hz. Hence, using the values of the field components (new) from figure 2, we evaluate the components of the Poynting's vector and show them in figure 3.

Figure 3 clearly shows the hugeness (in comparison with the CR-like SESR) of the effect of SESR-2Ω and also of SESR-4Ω. As compared to CR-like SESR (which is $<\sim$CR given out in the absence of the laser), the power output per unit area from SESR-4Ω is 10^{29}–10^{39} times larger and that from SESR-2Ω is 10^{44} times larger. The SESR-2Ω dominates considerably over SESR-4Ω by giving 5–15 orders of magnitude more power output per unit area. We note that the S_ϕ component is negligibly small as compared to the S_ρ and S_z components for SESR-2Ω. For SESR-4Ω, the component S_ρ dominates over the remaining two.

By considering the Gaussian cylinder of unit length and unit radius of cross-section with its axis coincident with the direction of the electron's motion, we calculate S, the power emitted in Gaussian units, as

$$S = (2\pi S_\rho + \pi S_z) \times 1.7035 \times 10^{-52} \text{ ergs (s cm)}^{-2}.$$

For the present situation specified in figure 3, the power emitted through SESR is calculated as $(S)_{\text{CR-like}} \sim 4.64 \times 10^{-44}$ erg s^{-1}, $(S)_{2\Omega} \sim 3.52$ erg s^{-1} and $(S)_{4\Omega} \sim 1.84 \times 10^{-6}$ erg s^{-1}. It shows that $(S)_{2\Omega} \gg (S)_{4\Omega} \gg (S)_{\text{CR-like}}$.

Here we note that the interaction of the electron possessing superphase motion with the counter-propagating laser gives rise to the SESR effect. As the laser considered in the example is pulsed, its pulse duration decides the time of the interaction. It may be in the range of micro- to pico-seconds, and so the electron energy considered in the above example (i.e. $\gamma_0 = 18.29$ which corresponds to 1.5×10^{-5} erg) can be seen to be quite sufficient to give such a large SESR-2Ω output (which may be in the range from 10^{-6} to 10^{-12} ergs per pulse).

3.4. Tunability

It may be possible to get variable output due to SESR (in terms of its frequency and intensity) by changing the external parameters such as electron energy (β_0, γ_0), laser frequency (ω_0), laser intensity (E_0) and refractive index (n_0) of the material. These four parameters provide a characteristic of 'tunability' to the SESR effect. Therefore, it is necessary to know the variation of the SESR w.r.t. these parameters.

In our earlier work [7] the variation of the SESR effect w.r.t. β_0, E_0, ω_0 and n_0 was studied separately in detail, and the conclusions drawn therein remain applicable for the present refined calculations also. As γ_0 is a preferred electron energy parameter, we study the variation of the SESR-effect w.r.t. it here. We also find the allowed electron beam energy ranges for different n_0-values.

The field amplitudes of the dominant components of SESR-2Ω are decided by the factors α_{18} and α_{13}. It may be seen that α_{13} is independent of γ_0, while α_{18} varies inversely w.r.t. γ_0. It implies that the SESR effect increases when electron energy is decreased (within the allowed range). It also is a very useful result because then the requirement to use higher and higher energy electron beams to get larger and larger outputs (in terms of frequency and power both) is not going to act as a limitation when SESR is used for that purpose. In all the existing radiation sources the electron beam energy needs to be increased as one wants to get the radiation of higher and higher frequency.

We note that the choice of the laser parameters E_0 and ω_0 should be such that $\beta_i \ll 1$ is satisfied. For a given dielectric n_0 is specified. By choosing μ ($\ll 1$) we find the required value of β_0 (satisfying $\beta_0 n_0 > 1$) because $\mu = (\beta_0 n_0 - 1)$. To estimate the SESR effect (specified by equations (19), (24)–(26)), we have considered the range of μ as (1×10^{-8}–1×10^{-2}), and have taken the n_0-values in the range of 1.000 0025–6, E_0-values in the range from 3 to 3×10^7 StatV cm^{-1} and ω_0-values in the range of 5×10^7–5×10^{16} Hz. We have included those values of E_0 and ω_0 which satisfy $\beta_i \leqslant 10^{-2}$. We show in figures 4(*a*) and (*b*) the maximum allowed electron beam energy values, $(E_b)_{\max}$ ($= 0.511 \times \gamma_0$ MeV), for different n_0-values which give the expected SESR effect along with the corresponding energy range ΔE_b in MeV. For a given value of n_0, the electron beam is expected to show the SESR effect in the range from $(E_b)_{\max}$ to $[(E_b)_{\max} - \Delta E_b]$. This range can be found from figures 4(*a*) and (*b*).

Thus, with the refined second-order calculations, we have shown that SESR is given out in the form of two components of frequency 2Ω and 4Ω which we named, respectively, as SESR-2Ω and SESR 4Ω. The SESR-2Ω is stronger than the SESR-4Ω and gives power output $\sim 10^6$ times that from SESR-4Ω. Each of these components is monochromatic, largely up-shifted w.r.t. laser frequency ω_0 $\left(10^3 < \frac{\Omega}{\omega_0} < 10^7\right)$, highly directional w.r.t. the direction of electron's motion (with $\theta = \tan^{-1}(1 - \frac{1}{\beta_0 n_0}) \to 0$), enormously amplified with power amplification $\sim 10^{27}$–10^{44} times that from the normal Cherenkov radiation (that may be given

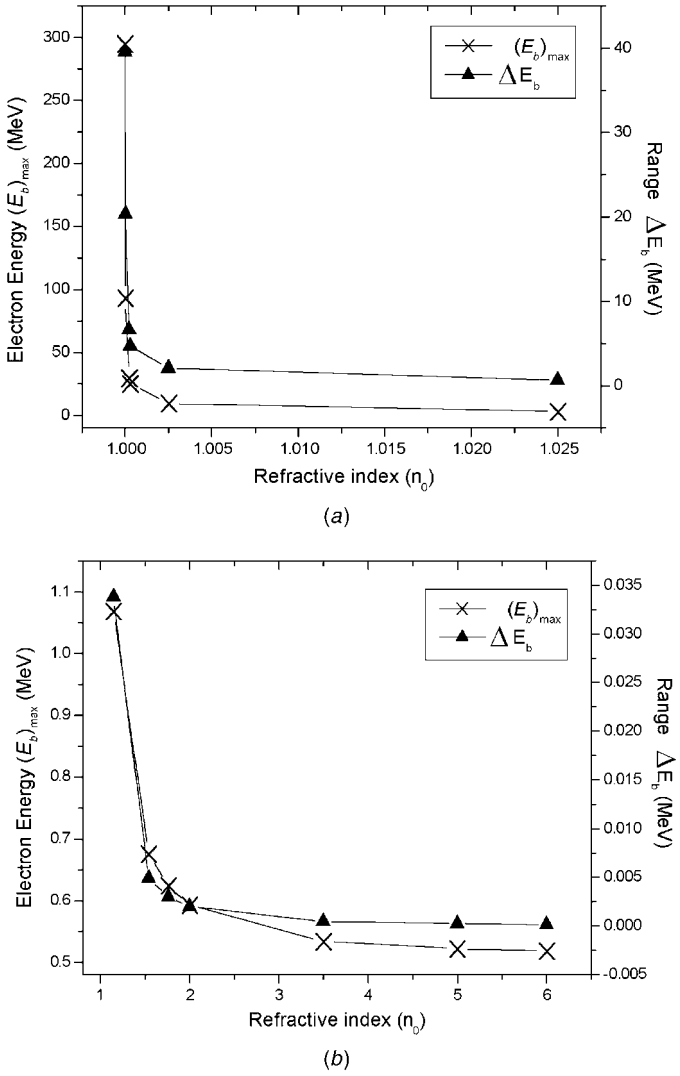

Figure 4. The maximum electron beam energy values $(E_b)_{\max}$ and the corresponding widths ΔE_b, both expressed in MeV, for which the SESR effect is possible for different n_0-values.

out in the absence of the laser, but under the same other conditions), coherent electromagnetic radiation which is also tunable.

All these interesting characteristics of SESR indicate a possibility of using it for the generation of high frequency, coherent electromagnetic radiation in the frequency region in which good sources, at present, are not available.

4. Conclusions

By using the classical, second-order, relativistic calculations, we have shown that very near to the threshold of superphase motion SESR is given out in the form of two monochromatic components of electromagnetic radiation showing the following characteristics:

(A) *Frequency output*. SESR-2Ω gives frequency $2\Omega \sim \frac{4\omega_0}{\beta_0 n_0 - 1}$, and SESR4Ω gives frequency $4\Omega \sim \frac{8\omega_0}{\beta_0 n_0 - 1}$. As compared to the incident laser, their frequency up-shifts can be very high, in the range of 10^3–10^9.

(B) *Directionality*. Both the components, SESR-2Ω and SESR-4Ω, are highly directional. Their emission is confined to the cone of half angle $\theta = \tan^{-1}\left(1 - \frac{1}{\beta_0 n_0}\right) \to 0$, w.r.t. the direction of the electron's motion.

(C) *Power output*. SESR-2Ω is stronger as compared to SESR-4Ω giving output power $\sim 10^6$ times more. It is enormously amplified with power amplification $\sim 10^{44}$ times larger compared to CR-like SESR and also to normal CR (that may be given out in absence of the laser, with the other conditions remaining unchanged).

(D) *Tunability.* SESR is tunable. The tunability is provided by the parameters ω_0 of the laser, γ_0 of the electron beam and n_0 of the material. SESR shows an increase with increasing E_0 and n_0, while it shows a decrease with increasing γ_0 and ω_0. However, the output power of SESR-2Ω is independent of ω_0.

Nevertheless, the SESR effect needs to be further investigated by considering the practical limitations for achieving the parameters taken as 'ideal' in our theory. The questions such as energy conservation, the SESR energy source (electron beam, medium or both) are required to be studied further in detail. The work in these directions is in progress and may be published elsewhere. At the same time the experimental work for its verification is very much required for further progress in this subject.

Acknowledgments

I would like to express my appreciation for the hospitality offered to me by Stanford University, USA during my stay as a visiting scholar at HEPL. I would also like to acknowledge the important contributions made by Professor Todd Smith of the Stanford Physics Department through many discussions that took place during my visit. Thanks are also due to the University of Pune for granting me a six months study leave to pursue this work at Stanford.

References

[1] Frank I and Tamm Ig C R 1937 *Acad. Sci. URSS* **14** 109
[2] Jelley J 1958 *Cherenkov Radiation* (London: Pergamon)
[3] Zrelov V P 1968 *Cherenkov Radiation in High Energy Physics* (Moscow: Atomitzdat)
[4] Becker W and McIver J K 1985 *Phys. Rev.* A **31** 783
[5] Pantell R H *et al* 1982 *Phys. Quantum Electron.* **9** 961
[6] Walsh J E 1982 *Phys. Quantum Electron.* **7** 255
[7] Risbud A A and Kamerkar N C 2001 *Phys. Rev.* E **63** 036501
[8] Arutyunyan V M and Avetisyan G K 1972 *Zh. Eksp. Teor. Fiz.* **62** 1639
Arutyunyan V M and Avetisyan G K 1972 *Sov. Phys.—JETP* **35** 854 (Engl. Transl.)
[9] Cohen L *et al* 1982 *NRL Memorandum Report* 4778 Naval Research Laboratory, Washington DC
[10] Schneider S and Spitzer R 1974 *Nature* **250** 643
[11] Schneider S and Spitzer R 1977 *Can. J. Phys.* **55** 1499
[12] Schneider S and Spitzer R 1977 *Appl. Phys.* **13** 197
[13] Schneider S and Spitzer R 1977 *IEEE Trans. Microw. Theory Tech.* **25** 551
[14] Schneider S and Spitzer R 1978 *Phys. Quantum Electron.* **5** 301
Schneider S and Spitzer R 1978 *Phys. Quantum Electron.* **5** 347
[15] Schneider S and Spitzer R 1980 *Phys. Quantum Electron.* **7** 323
[16] Zachary W W 1980 *Phys. Quantum Electron.* **7** 779
[17] Kroll N M 1980 *Phys. Quantum Electron.* **7** 355
[18] Soln J 1978 *Phys. Rev.* D **18** 2140

[19] Zachary W W 1979 *Phys. Rev.* D **20** 3412
[20] Becker W 1981 *Phys. Rev.* A **23** 2381
[21] Jackson J D 1975 *Classical Electrodynamics* 2nd edn (New York: Wiley) pp 552, 522–24, 513
[22] Risbud A A 1987 *J. Phys. A: Math. Gen.* **20** 2743
[23] Ginzburg V L 1961 *Propagation of Electromagnetic Waves in Plasma* (New York: Gorden and Breach) pp 226–28
[24] Frank I M 1968 *Sov. J. Nucl. Phys.* **7** 660
[25] Tamm I G 1939 *J. Phys. (Moscow)* **1** 439
Tamm I G 1939 *J. Phys. (Moscow)* **1** 446